Proceedings of ASME Turbo Expo 2011
GT2011
June 6-10, 2011, Vancouver, British Columbia, Canada

GT2011-45365

DESIGN AND TEST OF A SMALL HIGH PERFORMANCE DIAGONAL FAN

M. B. Schmitz
ebm-papst St. Georgen GmbH & Co. KG
St. Georgen, Germany

G. Eimer
ebm-papst St. Georgen GmbH & Co. KG
St. Georgen, Germany

H. Schmid
ebm-papst St. Georgen GmbH & Co. KG
St. Georgen, Germany

ABSTRACT

The development of two small high performance single stage diagonal fans is described. The design objectives and constraints are discussed and the aero-/acoustic performance of the new fan is compared to an existing diagonal fan.

For the aerodynamic design, the maximum flow coefficient and the maximum pressure coefficient at stall are prescribed together with geometrical constraints on outer diameter and axial space.

The aerodesign is carried out using a through-flow method and 3D CFD. Two design variants are presented, a design with guide vanes for pressure recovery and a variant with struts optimized for low noise. The numerical predictions are compared to experimental data. The agreement between the predicted performance and the experimental data is sufficient for design purposes. Compared to the existing diagonal fan, the new fan shows significant improvements in terms of efficiency, performance and noise without compromising versatility and overall dimensions.

INTRODUCTION

Compact fans are often used for cooling purposes in electronic applications such as telecom base stations. These applications are getting more and more compact, they are operated continuously and are often installed close to populated areas. For the cooling fans this means that there is an increasing demand for high air performance, high efficiency, small dimensions and low noise emissions. To ensure versatility, the fan should be able to get installed either downstream or upstream of the heat source, meaning blowing cold ambient air into the application or sucking hot air from the heat source towards ambient. To tailor the fan to a broad variety of applications, it is preferable when different motors can be installed into the hub, so different speed regimes can be realized. For this diagonal fan, the motor concept consists of an outer rotor and an inner stator that allows for small axial size but needs a relatively large hub diameter. For diagonal fans, this is not necessarily negative. The diagonal shape of the hub creates sufficient space to house motor and internal electronics.

For applications, where noise emissions are of minor importance but high pressure is required, like in paper industry, the increased demand on pressure is met by increasing the rotational speed of the motor. For those applications it is advantageous, to use guide vanes, which are able to recover some of the circumferential velocity.

Another design challenge of compact fans is their limited axial space. These fans are often used in installations with space constraints. This limits the design freedom, especially of the diffusion system and poses several challenges on the aerodynamic and acoustic design of compact fans.

The design goals and restrictions are described. The impeller design is done using a through-flow potential flow code and steady state 3D CFD. The vane design is done in a similar way, however the acoustic design is done mainly experimentally.

NOMENCLATURE

$\Psi_{st} = \dfrac{\Delta p_{st}}{\frac{\rho_1}{2} \cdot u_2^2}$: static pressure coefficient

$\Phi = \dfrac{\dot{V}_1}{\frac{D^2 * \pi}{4} * u_2}$: flow coefficient

$\eta_{stat} = \dfrac{\Delta p_{stat} \cdot \dot{V}}{\omega \cdot \mathrm{T}}$: static efficiency

$\eta_{tot} = \dfrac{\Delta p_{tot} \cdot \dot{V}}{P}$: total efficiency

$P = \omega \cdot \mathrm{T}$: mechanical power input$_t$

$\omega = 2\pi n$: angular speed

T_t : mechanical torque (as computed by CFD)

Δp_{st} : static pressure rise, free blowing

Δp_{tot} : total pressure rise

$\dot{V}_1$: volume flow at inlet

ρ_1 : density at inlet

$u_2 = \pi \cdot D_2 \cdot n$: circumferential speed

D_2 : outer diameter at exit

$v_{ax} = \dfrac{V_1}{A}$: flow velocity at exit

n : rotational speed

DESIGN REQUIREMENTS

The new fan family should fulfill the following requirements:

1. The maximum flow coefficient should be higher than 0.23 and the pressure coefficient at stall should be higher than 0.4 (Figure 1)

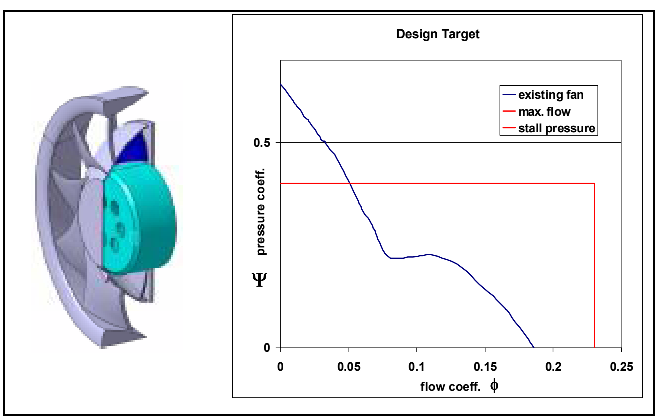

Figure 1: Mechanical concept (left), performance target (red) and existing diagonal fan curve.

With these design goals, the new fan should be able to deliver 28% more flow and 82% more pressure compared to the existing fan when operated at same rotational speed. Alternatively, similar performance could be achieved with significant lower speed. From an acoustic perspective, lower speed is preferred since the total sound power level SPL_t of fans depends on the rotational speed of the fan and on the specific fan type and size, the operation conditions and the quality of the aerodesign. All non-speed related factors could be expressed in form of the first term on the right side of eq. (1) [1], [2], [3].

$$\begin{aligned} &SPL_t = A^* + B \cdot \log(Ma) \\ &\text{with} \\ &Ma_2 = u_2 / a = \pi D_2 n / a \\ &a : \text{speed of sound at fan inlet} \end{aligned} \qquad (1)$$

In [4] it is shown, that flow-generated noise can always be described in the form of eq. (1). For fans it is useful to compute the Ma number from the circumferential speed at impeller tip u_2 and the speed of sound at inlet.

2. The new fan family should have the same outer dimensions than their predecessors, i.e. casing outer dimensions and overall axial length are given. In addition, the motor has to fit into the impeller hub (Figure 1, left). The selection of the motor determines the maximum possible speed up to which the fan can be operated, unless there are no other mechanical constraints. The outer diameter of the most powerful motor defines the minimum hub diameter. The prescribed maximum outer dimension of the casing defines the maximum shroud diameter. With these requirements, two impeller sizes can be deduced. A smaller impeller, with a relative impeller height of $t_{imp}/D_2 = 0.22$ and a larger impeller with $t_{imp}/D_2 = 0.27$. The two diagonal fans will be similar but aerodynamically not identical. Consequently, it is not possible to design only one fan and scale the geometry. In this paper, both designs are used to illustrate the aerodynamic design. The acoustic performance will be presented only for the small fan.

3. It should be possible to install the fan upstream and downstream in the application. The fan can be used to evacuate or to pressurize a plenum.

The design objective is, to optimize efficiency and minimize noise emission within the aforementioned constraints.

DESIGN PROCEDURE

To start the design loop, the rotational speed has to be prescribed as the input parameter. For compact fans this is a crucial point. Ultimately, the torque-speed capabilities of motor and power electronics define the maximum performance of the fan. The matching of the motor capabilities with the aerodynamic demands starts therefore right from the beginning of the fan design. For a given speed, the aerodynamic design sets the torque requirements for the motor, so a motor can be selected that has its best efficiency aligned with the best aerodynamic performance. This is strictly true for one speed line. In practice the motor will be adopted for every application that deviates significantly from the design speed.

Impeller Design

The early design requires methods that allow for quick design changes and fair estimations of torque and speed demands of the fan. The initial design is done with the commercially available inverse through flow method ADT1 [8] that assumes inviscid potential flow. The distribution of the circumferentially averaged swirl velocity rV_θ on the meridional plane of the impeller is prescribed and the corresponding blade shape is computed iteratively. The blade is represented by a sheet of vorticity with the strength of rV_θ. A detailed description can be found in ref. [11]. Zero vorticity is described at the leading edge and the vorticity distribution along the blade height at trailing is adjusted iteratively to meet the desired operation point. The blade is derived by assuming free-slip conditions and the blade thickness is taken into account as a blockage. This step yields reasonable estimations of flow channel shape, blade number and blade camber to meet a target design point. A rotational speed of 6000rpm has been prescribed. Figure 2 shows flow channel, the impeller geometry with nine blades and the blade pressure distribution for the larger fan ($t_{imp}/D_2 = 0.27$). The computed static pressure rise for this fan rotor is 750Pa.

The geometry obtained in this design step is taken as starting point for the 3D CFD design of the fan. The incompressible 3D Navier-Stokes equations are solved and more geometrical details like tip gap and casing geometry are taken into account. With 3D CFD it is possible to study the 3D flow inside the flow passage and downstream of the fan (Figure 3). For small axial and diagonal fans, the mixing losses downstream of the fan are the biggest contributors to the overall losses. For those machines, it is challenging to design effective diffusion systems because of their limited axial dimensions.

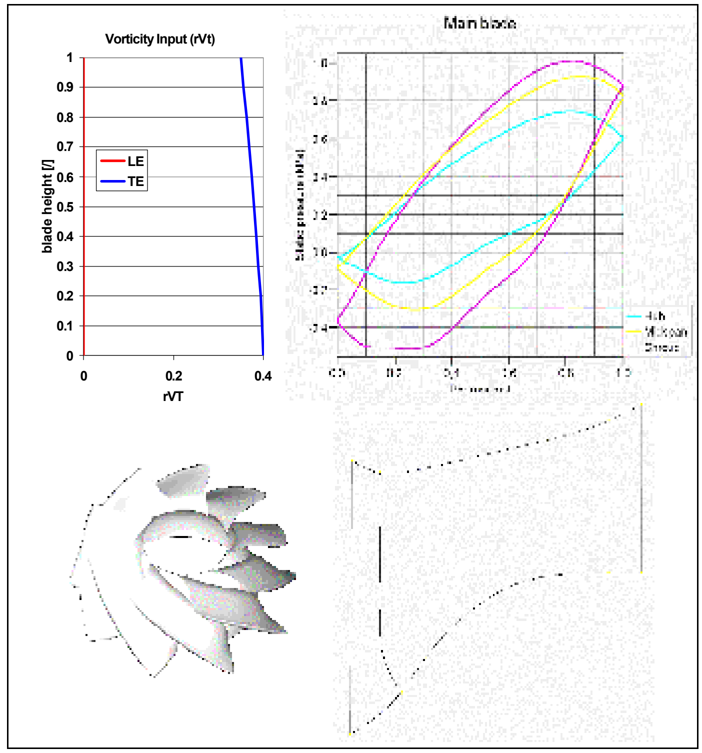

Figure 2: Flow channel and calculated gauge blade pressure distribution.

The commercial CFD solver STAR-CCM+ ,[9], is used to compute the flow field for at least three different operation points along the fan characteristics. The computational domain simulates the test rig conditions, i.e. the actual set up of the suction side throttled in-house facility (Figure 12) is modeled. The numerical set-up is shown in Figure 3. One blade sector is modeled with 1.2 million polyeder cells, the impeller region is resolved with 780k cells and prism cells are applied to the wall boundary layer which is resolved with four prism cells. The realizable $k\varepsilon$ turbulence model in connection with the two layer all y+-model is used for the calculations. With these settings, the tip gap of 0.8mm width could be resolved with 11 to 14 cells (lower picture in Figure 3). A detailed description of the numerical method, mesh algorithm and code itself can be found in ref. [9]. The fluid velocity is prescribed at inlet, the exit is modeled as pressure outlet. The actual speed of revolution is applied to the simulation in order to compute the required blade torque. This information is then used to assess possible motors and electronic solutions.

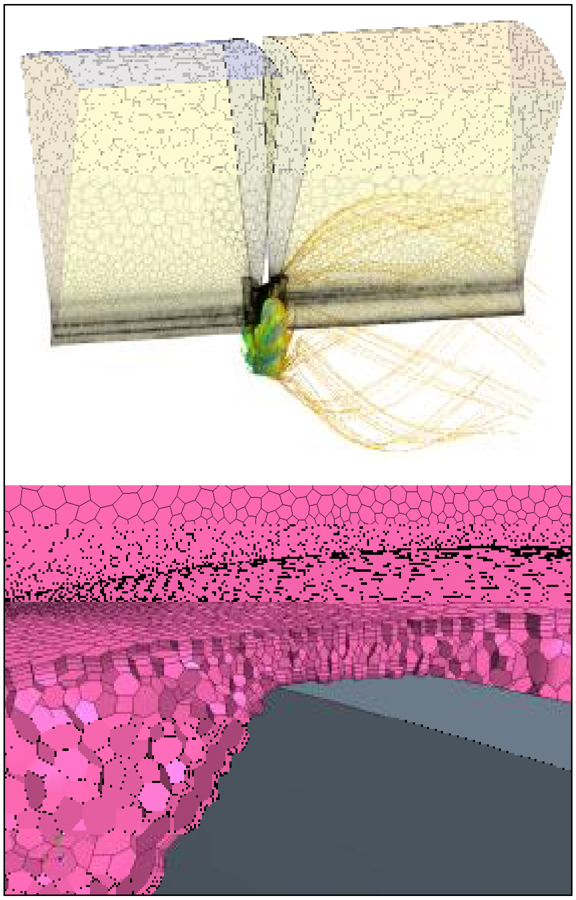

Figure 3: Upper picture: computational domain and streamlines at design point. Lower picture: grid structure of tip gap region.

The CFD results are used for further (manual) design iterations. The main objective in this step is to optimize the (static) efficiency η_{stat} at design conditions without compromising the maximum operation range or the stall point. In Figure 3, the streamline indicate the flow behavior for free outflow conditions, the corresponding total pressure is shown in Figure 7. In

Figure 4 and Figure 5, the velocity vectors, static pressure and relative velocity contours are presented on blade-to-blade cuts through the impeller. The data refers to the design point of the smaller fan. The right picture in

Figure 4 indicates the reference plane downstream of the impeller that is used to compute the required impeller efficiency values. The velocity data is extracted at this position and the circumferentially averaged velocity profiles are computed. These profiles are used to design guide vanes and struts.

In the CFD visualization a difference in flow angle and blade angle can be seen. The profiles of the guide vanes and struts are designed with respect to this behavior.

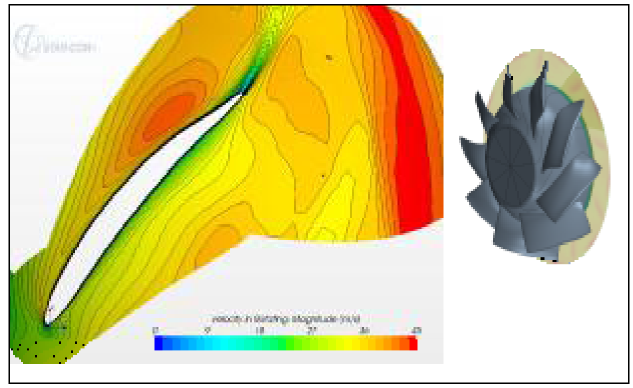

Figure 4: Flow field of the small fan without struts.

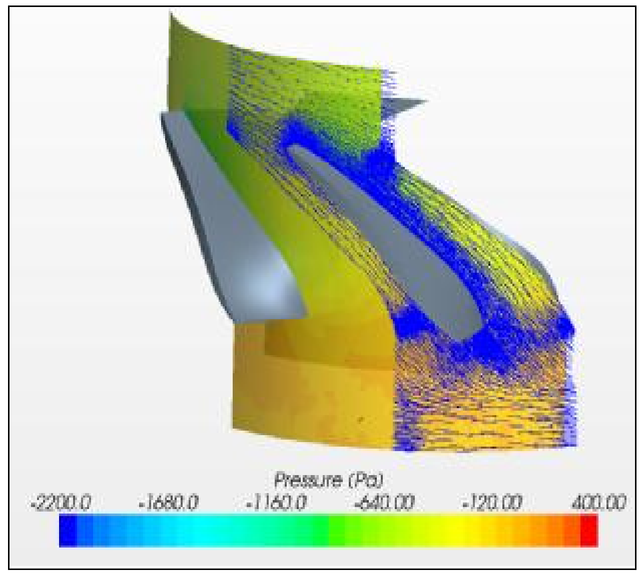

Figure 5: Gauge static pressure and flow vectors of the relative velocity on a blade-to-blade surface through the impeller

In Figure 6 the velocity in the rotating system is shown for the smaller impeller at design conditions. The effect of the tip gap flow from pressure to suction side is clearly visible. The tip vortex and its interaction with the neighboring blades and downstream vanes is one major source of flow-induced noise. In this design, the blade loading is chosen such that the roll up of the tip vortex is pushed to a more downstream position in order to mitigate noise and to maintain high blade efficiency.

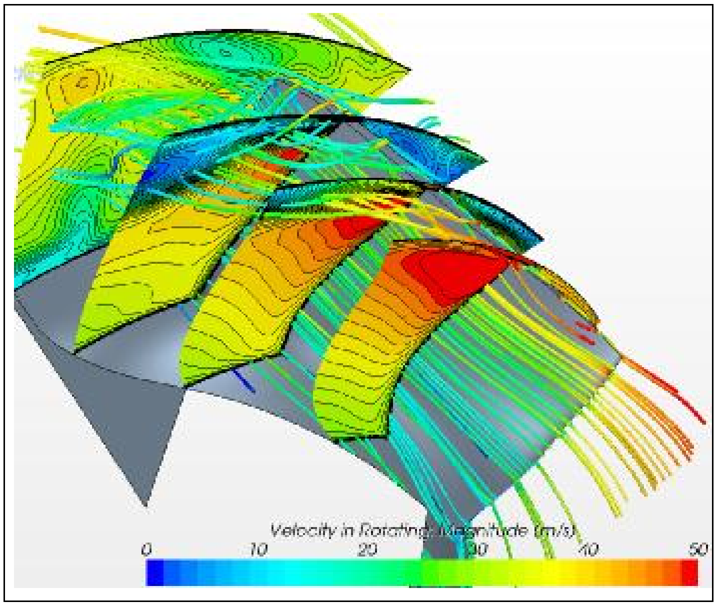

Figure 6: Flow field through the impeller.

In Figure 7 the flow downstream of the fan is visualized for the same operation point. The flow exits into ambient. The picture gives an indication of the flow and loss development downstream of the fan stage. Because of the limited axial space, there is no option to apply a long vaned diffuser. Adding guide vanes downstream of the impeller can reduce the losses due to uncontrolled diffusion.

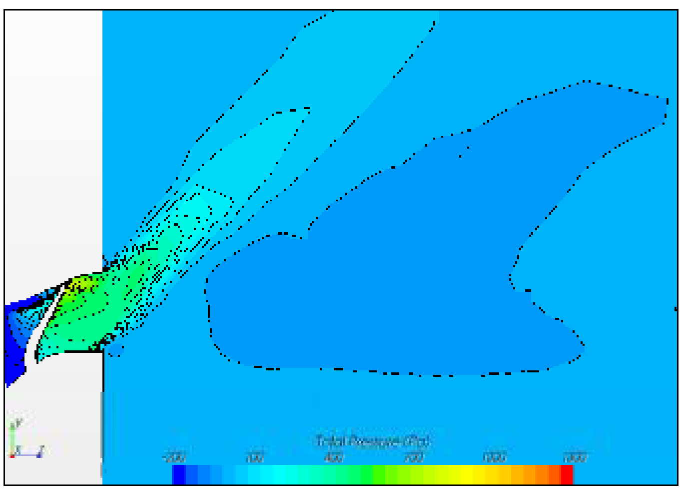

Figure 7: Flow field downstream of the fan.

In the next step, the design of these guide vanes and struts is briefly described.

Vane Design

Often, struts of compact fans are designed mainly due to mechanical restrictions and optimized for minimum noise emissions. Their main function is to connect the back flange with the motor and the impeller mechanically to the casing. However, for pressure demanding applications guide vanes to recover some of the dynamic pressure of the exit swirl can replace the struts. Therefore, two versions of struts are designed. One version is optimized for highest static pressure recovery and another strut design is presented for best acoustic performance. The mass flow averaged velocity profiles at impeller exit (Figure 8) are extracted from the CFD solution and used as input for the strut and guide vane design, which is done again using the through-flow method.

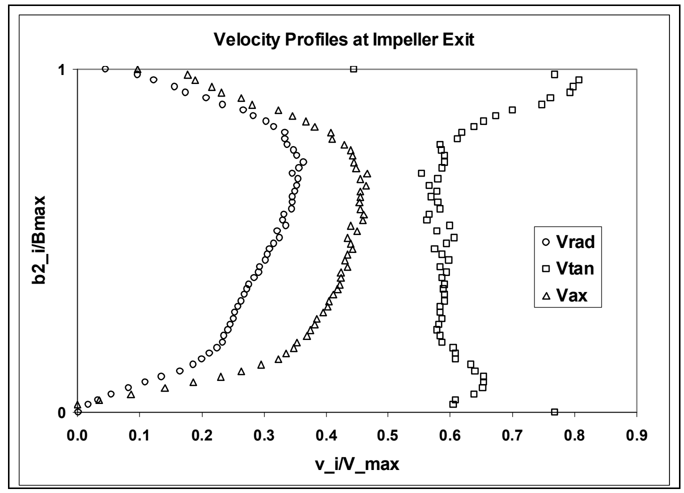

Figure 8: Circumferentially averaged velocity profiles at impeller exit.

With the through flow code, each blade row is designed independently. Vane number, axial position, vane stacking and chord length are varied to achieve either high pressure recovery or low noise emissions. The guide vanes should recover swirl and transfer it to static pressure or axial velocity. They are designed for high flow turning. The struts should not increase the overall sound power level meaning they should not disturb the flow field. Ideally, they are neutral structures without creating recirculation areas or increasing turbulence. With these design objectives, the vane geometries are designed with the through-flow code and the results are used as starting point for the detailed design with 3D CFD. Here, blade row interactions are taken into account via a mixing plane interface. In addition to the CFD studies, a complementary test campaign is conducted.

Figure 9 shows the actual designs of the new diagonal fan. The guide vanes for pressure recovery are positioned as close as possible to the impeller exit. Sufficient chord length is required to achieve the necessary turning. It has been found that five vanes (Figure 9, right picture) give best aero performance and ensure mechanical integrity.

Figure 9: Impeller (left) and performance optimized (right) guide vanes.

In Figure 10 the effect of the guide vanes on the efficiency is shown for the large fan stage. The leading edge of the impeller is taken as reference position. The 100 percent value corresponds to a mechanical power input of $P = \omega \cdot \mathrm{T}_t$, where the torque T_t is extracted from the CFD results. This value is taken as reference to compute the total efficiency η_{tot} between impeller leading and trailing edge, fan stage exit and far downstream of the fan [5]. According to Figure 10, the guide vanes increases the losses in the fan stage but are able to reduce the mixing losses downstream thereby causing an overall total efficiency increase.

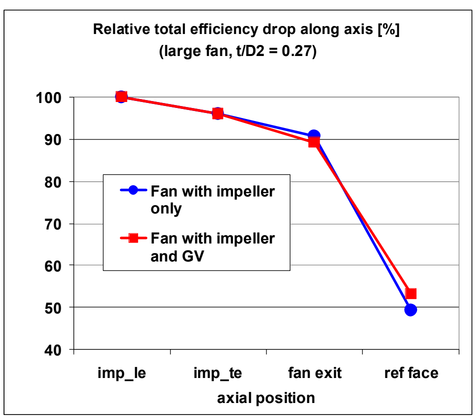

Figure 10: Effect of guide vanes on total efficiency (large fan, design point).

Experimental Set-Up

The experiments focus on fan charts and sound power level. A modular experimental test set-up is developed that consists of the four major fan components casing, impeller, struts and motor. Each of these components can be exchanged individually to study its particular influence on the overall performance. In this campaign, only the aerodynamic components (vanes and impeller) are exchanged.

Figure 11 shows the experimental set-up that is used for all experiments. The impeller with its motor is connected to a back plate via mechanical holders (rods and struts) that are placed sufficiently far downstream to not interfere with the exit flow. This modular configuration allows for quick exchange of struts and guide vanes. Even a benchmark case without struts or guide vanes can be constructed. The aerodynamic components are made by rapid prototyping.

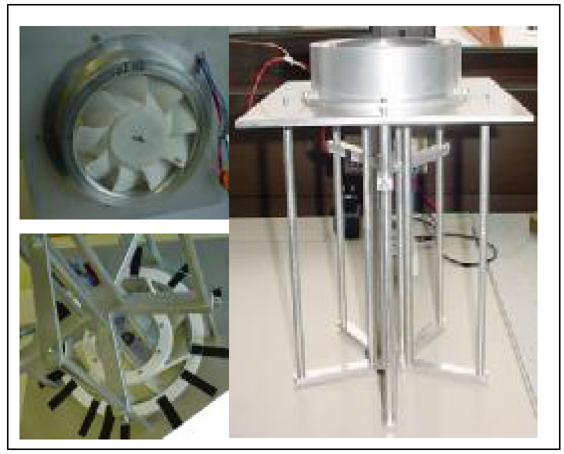

Figure 11: Experimental set-up.

Beside its modularity, the test set-up can be used to determine the air performance as well as the acoustic behavior of the fan. The disadvantage of this installation is, that motor and aerodynamic effects are difficult to separate. To assess different aerodynamic configurations with respect to their efficiency, the motor efficiency of the test object must be known. The motor used for this study has efficiencies between 80% and 85% in the investigated speed range.

The aerodynamic test rig (Figure 12) is a suction side throttled facility. The test object is mounted at the test chamber exit, the inlet flow is conditioned with screens and gauzes to ensure homogeneous flow at the fan inlet. The air enters the rig via five tubes, each equipped with a flow meter. An auxiliary fan compensates the pressure drop in the system. The fan exit is at ambient, the static pressure difference in the inlet chamber against ambient is recorded. In the acoustic test rig (Figure 12, right picture) the fan is throttled from the pressure side. The total sound power is computed according to ISO10302 with ten microphones placed on a sphere with a two-meter diameter.

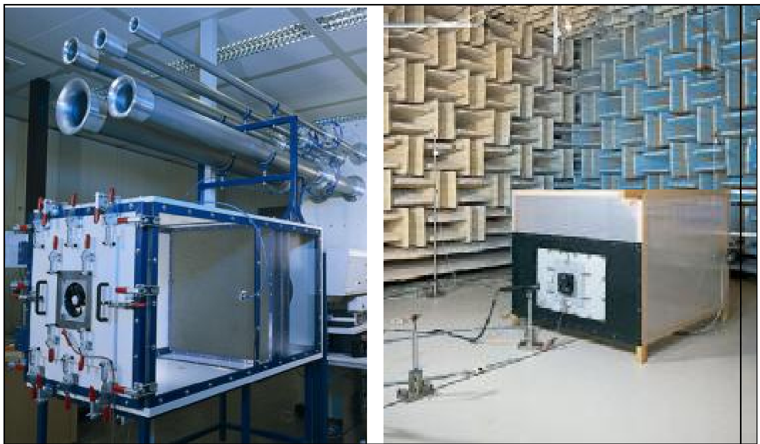

Figure 12: Aerodynamic (left, [6]) and acoustic (right, [7]) test rigs.

To get reliable acoustic data, the mechanical parts are kept identical, i.e. the same motor and the same electronics are used in every acoustic experiment. Nevertheless, the combination of a prototype motor with a new aerodynamic configuration poses several challenges on the acoustic assessment. For higher speeds, the aerodynamically generated noise will be the dominant noise source [1], [2], but for smaller speeds the noise generated by a high-performance motor is significant. Furthermore, the material of the prototypes differs from the plastic material of the final product, which means that the mechanical and the acoustic properties will differ from the prototype to the final product. The noise, generated by the fairly rough surface of the prototypes will reduce when using a production fan with the final material and the final manufacturing process. This has to be taken into account, when comparing the test results to the data obtained on a production product.

AERODYNAMIC PERFORMANCE

In Figure 13, the aerodynamic performances of the fan stages are presented. Additionally, in Figure 13 the comparison to CFD is shown for the larger fan. The agreement of the CFD simulations with experiments is good. The blue dots in the right picture of Figure 13 are results of three CFD calculations of impeller and casing and the red point is the result of a mixing plane calculation of the full stage with guide vanes. The good agreement between predictions and experiments can partly be explained with the homogeneous inflow conditions in the test rig, which are close to the ideal situation in the CFD simulation.

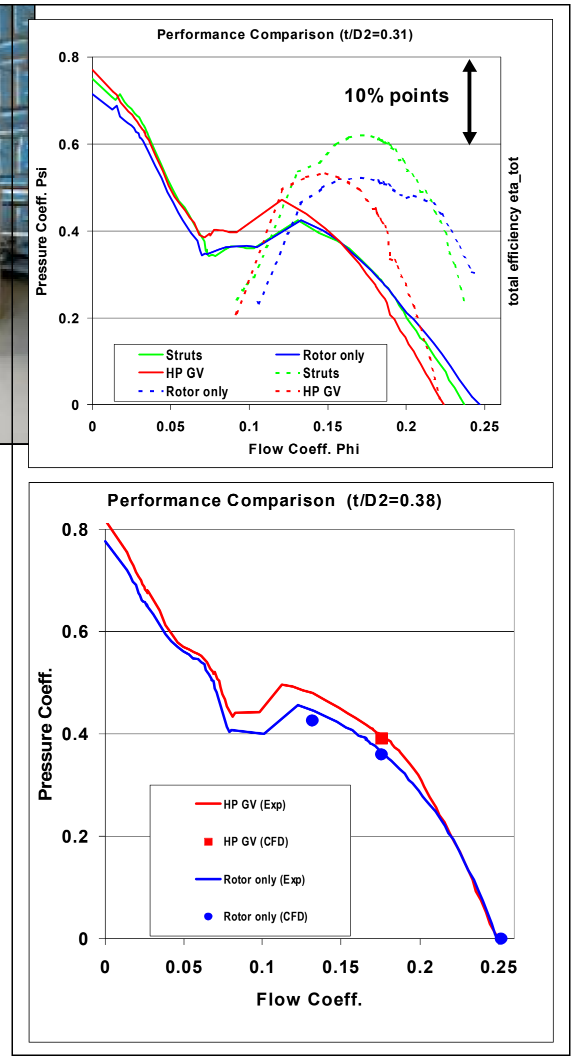

Figure 13: Aerodynamic performance and comparison to CFD.

The guide vanes increase the static pressure of about five points. For the smaller fan, the blockage of the guide vanes compromises the maximum flow rate and shifts the useful operation range toward smaller flows, while for the larger fan, no flow reduction is measurable (red curves in Figure 13). The left part of Figure 13 shows the performance of the smaller fan stage. As for the larger fan, the results are compared to the values of the solo impeller. The green line is the performance chart for the stage with the noise-optimized struts. Those struts reduce the flow rate very little, compared to the guide vanes (red line, left picture of Figure 13). The increase of total efficiency can be explained with reduced mixing losses downstream of the impeller. Apparently, the struts mainly straighten the flow and increase the axial velocity (at design conditions), which in turn results in improved total efficiency. The guide vanes transform swirl to static pressure thereby reducing the axial velocity.

ACOUSTIC CHARACTERIZATION

The design strategy for acoustically optimized struts is to disturb the downstream flow field as least as possible. For fixed geometries, this can only be achieved at a single operation point, for off-design conditions the strut profile will perform less effectively i.e. they will generate more audible flow turbulence. It is therefore of interest to design the struts for a broad operation range. In this study, seven different strut designs have been investigated, all were designed using the impeller exit flow as shown in Figure 8. The main parameters of the strut profiles are shown in Table 1.

	V1	V2	V3	V4	V5	V6	V7
#	4	4	7	4	4	4	4
gap	large	small	large	small	small	small	small
max. thicknes s	-	-	-	+	+	+	+

Table 1: Strut design, parameter variation.

V1 to V7 denotes variations in camber lines and staggering. Stator sets with seven or four struts have been investigated ('#' in table 1), with more (+) or less (-) maximum profile thickness. The leading edge of the strut has been placed with a large or small gap downstream of the impeller (Figure 14), thereby keeping the overall axial length of the fan stage the same for all variants.

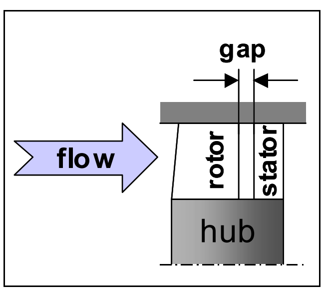

Figure 14: Rotor and stator gap.

The results of this investigation are summarized in Figure 15. The increase of the overall sound power level with respect to the sound power level of the fan without struts is shown.

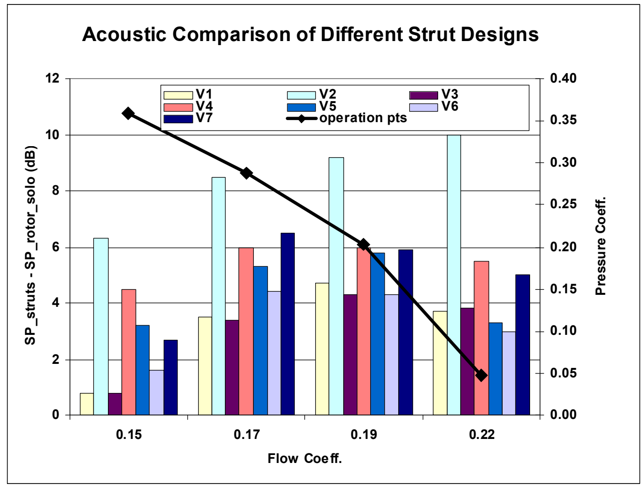

Figure 15: Sound power of different strut design for four operation points.

For this particular diagonal fan design, the strut variants V1 and V3 show best acoustic performance in the preferred operation range. V2 with small thickness and positioned close to the impeller exit has the highest noise emissions. The high variation in the sound power levels shows the importance of a careful strut design. Strut design V3 (Figure 16) is selected for the final fan stage because of its good acoustic behavior and the preferable mechanical properties.

Figure 16: Noise optimized struts.

To compare the noise emissions of the new diagonal fan to the existing design, both fans are operated in the acoustic test rig with two different but constant throttle settings. For each setting the speed is changed, which means the fan operates at the same dimensionless operation point along the system impedance. Two system impedances are selected for which both fans operate close to or exactly at their best performance (Figure 17, left picture). For identical throttle settings (operation either along the solid or dashed system impedance curve) each fan is operated at the same operation point, i.e. it delivers the same flow rate. The increasing static pressure on the x-axis of the right picture in Figure 17 is the results of speeding up the fan along the system characteristic.

In the right part of Figure 17, the results of the four experiments are shown. The circles denote the new diagonal fan, the square symbols stand for the sound power level data of the existing design. Generally, the new fan has less noise emissions compared to the existing model. Especially for higher speeds the differences between the two fans increase, reflecting the improved aerodynamic shape of the new fan.

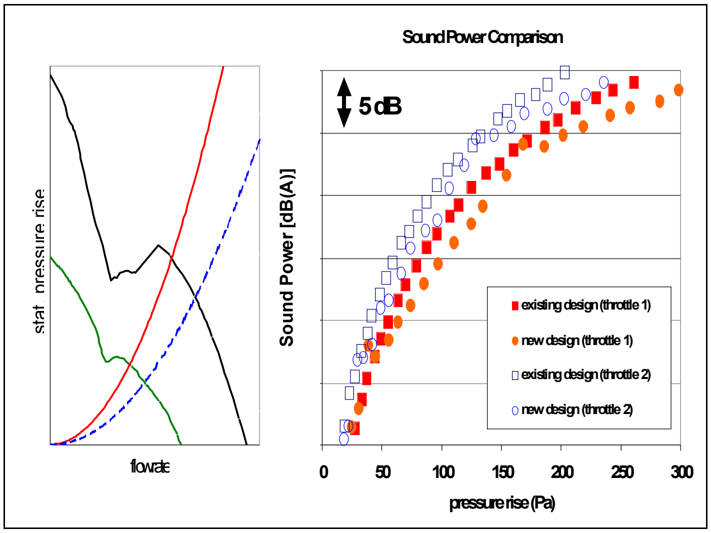

Figure 17: Sound power comparison along two system impedances.

SUMMARY

The design of a new family of compact diagonal fans has been described, the aerodynamic and acoustic behavior has been characterized and assessed. 3D CFD has been used to define the aerodynamics of the new fans while the aeroacoustic design of the struts has been done mainly experimentally. The new aerodynamic concept shows substantial improvements compared to the conventional diagonal fan design. The design goals in terms of flow rate and pressure rise could be achieved and the noise emissions could be reduced compared to the existing fan design. The total aerodynamic efficiency is increased by 10% with respect to the existing design (Figure 18). The new fan designs are the basis for a family of new diagonal fans. In the next steps, the design features will be transferred to diagonal fans with even smaller dimensions.

ACKNOWLEDGMENTS

The authors would like to thank M. Weiß and R. Haermeyer for their contribution.

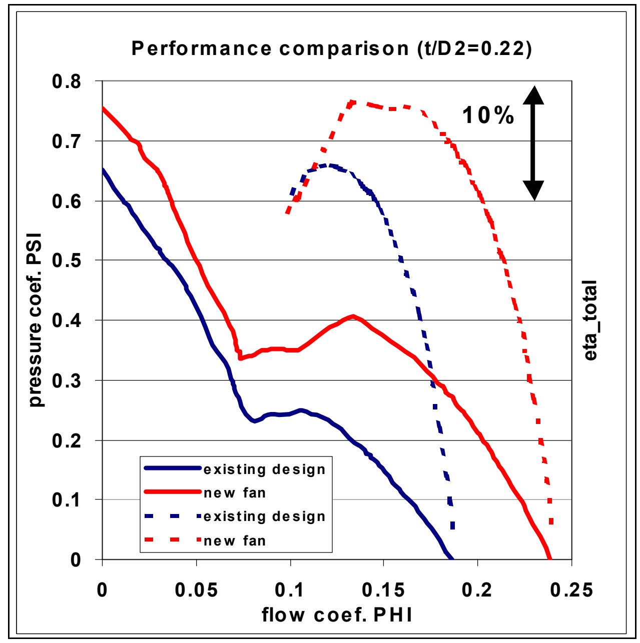

Figure 18: Performance comparison of the new and the existing diagonal fan.

REFERENCES

[1]. Bommes, et. al, Ventilatoren, Vulkan Verlag, Essen

[2]. Carolus, T., Ventilatoren-Aerodynamischer Entwurf, Schallvorhersage, Konstruktion, Teubner Verlag, Stuttgart

[3]. Regenscheid, B.: Die Schallerzeugung von Ventilatoren, in Eck, B., Ventilatoren, Springer-Verlag, 1972

[4]. Grundmann, R., u. Kramer, C.: Einheitliche Darstellung von Strömungsgeräuschen HLH Bd. 42 (1991) Nr. 3, S. 233/38 (Teil 1) und Nr. 4, S. 275/81 (Teil 2).

[5]. W. Bohl, Ventilatoren, Vogel Buchverlag, Würzburg, Germany, 1983.

[6]. Fans; performance testing, standardized test airways, DIN 24163, part3

[7]. Acoustic Method for the measurement of airborne noise emitted by small air moving devices, ISO 10302

[8]. ADT, Turbo Design1 Manual, 2009

[9]. CD-Adapco, STAR-CCM+ Version 4.02 User's Manual 2009.

[10]. W. Laufer, Finite-Elemente Modell zur rotordynamischen Berechnung von Ventilatoren, VDI Fachtagung Ventilatoren, Braunschweig, Germany, 2010

[11]. Zangeneh, M. , 1991, A Compressible Three-Dimensional Design Method for Radial and Mixed Flow Turbomachinery Blades, Int. J. Numerical Methods in Fluids, Vol. 13, 1991, pp. 599-624.